Online Sensorless Induction Motor Temperature Monitoring

Maximiliano O. Sonnaillon, *Member, IEEE*, Guillermo Bisheimer, Cristian De Angelo, *Member, IEEE*, and Guillermo O. García, *Senior Member, IEEE*

***Abstract*—A sensorless internal temperature monitoring method for induction motors is proposed in this paper. This method can be embedded in standard motor drives, and is based on the stator windings resistance variation with temperature. A small ac signal is injected to the motor, superimposed to the power supply current, in order to measure the stator resistance online. The proposed method has the advantage of requiring a very low-level monitoring signal, hence the motor torque perturbations and additional power losses are negligible. Furthermore, temperature estimations do not depend on the knowledge of any other motor parameter, since the method is not based on a model. This makes the proposed method more robust than model-based methods. Experimental results that validate the proposal are also presented.**

***Index Terms*—DSPs, induction motor drives, induction motor protection, signal injection, temperature measurement.**

I. Introduction

THIS PAPER deals with online monitoring of induction motors internal temperature. Typical applications are motor protection from overheating, capability to generate over-torque for limited periods, and correction of motor model parameters.

The most typical application of temperature monitoring is for protection purposes. Operating electric motors at temperatures higher than the nominal during long times can affect the windings' insulation, producing motor life-time reduction or even irreversible damages. The main causes of temperature increment are cooling-system failures and excessive currents through windings [1].

A second possible application of temperature monitoring is over-torque generation. In steady-state operation, the motor maximum torque is limited by its power dissipation capability. The motor thermal time constants are much longer than the electrical and mechanical ones. Hence, a current higher than the nominal one can be supplied during a limited time in order to generate over-torque without producing motor overheating. The periods are limited by the motor internal temperature. This over-torque capability is important in applications, where high torque with reduced duty cycle is needed (e.g., robotics). In these applications, it is mandatory to know the actual internal temperature to avoid motor damages.

Another usual application that needs temperature monitoring is in high-performance controllers. Temperature variations affect the motor drive controller performance when it uses estimators [2]. The knowledge of the actual motor temperature allows correcting the parameters' values, thus avoiding estimation errors due to temperature changes (e.g., the stator resistance can vary between 80% and 150% of its nominal value [2]).

In many electric drives, the internal motor temperature is measured using sensors placed inside the windings. These sensors can be thermocouples, thermistors, or devices based on semiconductors. The sensors and their acquisition system may have an important impact in low-cost applications. Moreover, temperature sensors must be installed inside the motor during the assembling process. Hence, it is complicated to measure the temperature of electric motors without sensors installed by the manufacturer or without a further disassembly to mount them. Sensor cables between the motor and its controller can also present troubles in case of hostile environments (e.g., electromagnetic noise) or can make the drive installation difficult.

For the aforementioned reasons, it is desirable in many cases to avoid temperature sensors and estimate, instead the motor temperature using already available measurements.

Temperature estimation methods based on thermal and electromagnetic motor models are found in literature [3], [4]. However, these methods fail when the model changes, for instance, due to cooling system failures or its dependence on operating conditions (e.g., fan speed).

Stator temperature monitoring is enough to protect low-power squirrel-cage induction motors, since the stator windings present the most frequent overheating problems [5]. Furthermore, in low-power drives, the temperature sensor elimination has a more significant impact in the overall system cost.

The average stator windings temperature can be estimated by using its electric resistance measurement and the copper resistivity dependence with temperature. Hence, an online stator resistance measurement technique can be used to monitor the motor internal temperature during normal operation.

If the rotor temperature is required (e.g., for high-power motor protection), it can be estimated from the stator temperature. A stator temperature monitoring method can be combined with a thermal model [6] or a rotor resistance estimation method [7] in order to obtain the temperature of both windings.

The main objective of this paper is to propose a simple low-cost strategy to monitor the stator winding temperature of induction motors online. The strategy is based on the stator winding resistance measurement accomplished by the motor controller.

Manuscript received January 16, 2007; revised May 20, 2007; accepted May 25, 2007. Date of publication March 22, 2010; date of current version May 21, 2010. This work was supported by the National University of Río Cuarto, Agencia Nacional de Promoción Científica y Tecnológica, and Consejo Nacional de Investigaciones Científicas y Técnicas. Paper no. TEC-00005-2007.

M. O. Sonnaillon is with Elgar Electronics (now AMETEK Programmable Power), San Diego, CA 92121-2267 USA (e-mail: msonnaillon@ieee.org).

G. Bisheimer is with the Department of Electrical and Computer Engineering, University of the South, Bahia Blanca 8000, Argentina.

C. De Angelo and G. O. García are with the Applied Electronics Group, National University of Rio Cuarto, Rio Cuarto 5800, Argentina.

Digital Object Identifier 10.1109/TEC.2010.2042220

The stator winding resistance measurement is performed by injecting an ac signal with very low amplitude and low frequency. An embedded digital lock-in amplifier (LIA) [8] is used to accurately measure the low frequency current and voltage drop in the stator windings. From these measurements, the stator resistance is computed and the temperature is estimated. The method only requires phase voltages and currents measurements, which are generally available in modern motor drives. The main advantage of this proposal is that it requires the injection of a very low level signal, improving the already published works.

The paper is organized as follows. First, existing methods are analyzed and their disadvantages are exposed. Then, the proposed method is described and the measurement technique details are given. The injected current effects on motor operation are analytically studied. In Section III, the implemented prototype used to obtain experimental results is described. In Section IV, experimental results that validate the correct operation in different operating conditions are shown. Finally, conclusions are drawn and a short discussion about the applicability of the proposed method is presented.

II. Existing Methods

A. Model-Based Methods

Stator resistance can be estimated using algorithms based on electromechanical models [9]. This type of estimation is very sensitive to model errors, making temperature estimations not robust [10]. Recently, Wu and Gao [11] proposed a stator and rotor temperature estimation method that combines ac signal injection with a motor model strategy. This method has the aforementioned problem: it is based on a simplified (linear) equivalent circuit. Hence, temperature estimations are not robust against parameter variations (e.g., due to iron saturation or skin effect) or model uncertainties.

Milanfar and Lang [6] proposed a thermal model combined with temperature sensors, placed in accessible locations, used to estimate temperature-dependent motor parameters. The main advantage of this proposal is the capability to estimate the temperature of motor locations, where it is difficult or costly to mount sensors. (e.g., rotor). The disadvantage is that it requires specific sensors placed inside the motor (e.g., stator windings) and it depends on the thermal model validity.

B. Signal Injection Methods

Direct stator resistance measurement allows temperature estimation without dependence on thermal, electromechanical, or any approximated model. Furthermore, the temperature monitoring system is simpler, it requires lower real-time processing and does not need any motor parameter to operate.

The most common technique used to measure the stator resistance online is dc injection. Holliday *et al.* [12], De Souza Ribeiro *et al.* [13], and recently Stiebler and Plotkin [14] have proposed schemes, where a small dc current is superimposed to the power supply current using the motor drive inverter. Lee and Habetler [5], [15] proposed monitoring the internal temperature of line-connected induction machines by using an external device connected in series with one of the motor phases. This device adds a dc component to phase voltages and currents, and measures them to estimate the stator resistance. In [5], they evaluate and correct possible temperature estimation errors produced by power cables resistance and other resistive components connected in series with the machine windings.

Injecting extra signals to the machine, as in the former proposals, produces negative effects, such as power looses increment, torque distortion, and machine magnetic saturation increment. For these reasons, it is desirable to measure the stator resistance with the lowest injected current amplitude as possible.

The main limitation of measuring small amplitude dc signals is imposed by offset and drift in the analog circuits. Although these problems can be reduced using high precision integrated circuits, they cannot be completely eliminated (e.g., due to unknown sensor offset). For example, Lee and Habetler report limitations in their proposed scheme due to the analog circuits offset and drift [15]. Their temperature monitoring system is able to estimate temperature accurately in steady state, but not during motor transients. In [14], the temperature estimation accuracy is also limited by offset in the measured signals.

Based on the preceding discussion, it can be concluded that the main problem to solve is how to accurately measure the stator resistance by injecting a very low-level signal, thereby making the secondary effects negligible. Solving this problem would make these types of strategies really attractive for industrial applications.

III. Proposed Method

The resistivity dependence on temperature of many materials is traditionally used as a temperature transducer. It is used to transform the physical variable temperature into a parameter that can be electrically measured. The most common devices are thermistors with positive temperature coefficient (PTC) or negative TC (NTC). These sensors are widely used in electric machine temperature measurement due to their robustness and simplicity.

The method proposed in this paper uses the resistivity variation with temperature of the stator windings, which are usually made of copper. This variation is approximately linear, and can be described by the following equation:

$$T = T_0 + \frac{R - R_0}{\alpha R_0} \tag{1}$$

where α is the temperature coefficient, approximately equal to 3.82×10^{-3} 1/°C for copper. The variables R and T represent the copper resistance and temperature, respectively, and the subindex 0 indicates the initial state.

Modern electric drives require an initial configuration procedure before the first operation. In this initialization, the motor electric characteristics are entered by the user and the electric drive performs an automatic parameter measurement (self-commissioning). The proposed method requires a manual measurement of the motor temperature (T_0), while the motor drive measures the corresponding stator resistance (R_0). This temperature can be obtained by measuring, after a long-enough

time with the motor turned off, the room temperature near the motor.

Using (1) and the copper temperature coefficient, the measurement accuracy requirements can be computed taking into account the desired temperature estimation accuracy. For instance, for overheating protection purposes 10 °C is an acceptable precision. This represents less than 10% the stator windings maximum temperature variation, from 25 °C (room temperature) to 130 °C (maximum recommended temperature for class B insulation).

Considering the minimum required precision, the stator resistance should be measured with the following maximum error:

$$e_R(\max) = e_T(\max)\alpha \approx 3{,}82\%. \tag{2}$$

The measurement method must guarantee that the R_S measurement error does not exceed this value.

A. Measurement Method

As previously mentioned, proposals that measure R_S online by injecting a small dc current are found in literature. The main problem of using small dc signals is the analog circuits' offset and drift. These factors reduce the measurement precision if the signal levels are too low. A simple solution to this problem is the utilization of ac instead of dc, hence offset and drift effects do not affect the measurements and the signal level can be significantly reduced. As the signal level is reduced, its negative effects (e.g., power losses and torque distortion) are also reduced.

In this paper, a small ac signal is used to measure the stator resistance online. The measurements are performed by using the synchronous detection technique, used in LIAs [8].

LIAs are measurement instruments designed to measure small ac signals in presence of noise with much higher levels. An LIA uses a sinusoidal reference signal $r_X(t)$, and its quadrature version $r_Y(t)$

$$\begin{aligned} r_X(t) &= \sin(2\pi f_0 t), \\ r_Y(t) &= \cos(2\pi f_0 t). \end{aligned} \tag{3}$$

The input signal $i(t)$ is composed by a sinusoidal signal of frequency f_0 added to a generic function that represents noise and harmonic distortion called $n(t)$

$$i(t) = A\sin(2\pi f_0 t + \theta) + n(t). \tag{4}$$

A digital LIA amplifies and digitizes this signal. The processing software multiplies the input signal by the in-phase and quadrature (shifted 90°) reference components

$$\begin{aligned} p_X(t) &= i(t)\, r_X(t) \\ &= \frac{1}{2}A\cos(\theta) - \frac{1}{2}A\cos(4\pi f_0 t + \theta) + n_X(t) \end{aligned} \tag{5}$$

$$\begin{aligned} p_Y(t) &= i(t)\, r_Y(t) \\ &= \frac{1}{2}A\sin(\theta) + \frac{1}{2}A\sin(4\pi f_0 t + \theta) + n_Y(t) \end{aligned} \tag{6}$$

where $n_X(t)$ and $n_Y(t)$ represent the noise functions after the multiplications.

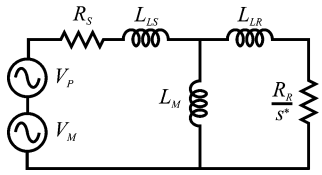

Fig. 1. Induction motor steady-state equivalent circuit with two voltage sources. The slip is different for each frequency.

Filtering-out the ac components and keeping the average value (dc signal), two signals with estimations of the in-phase (real) and quadrature (imaginary) components of the input signal are obtained

$$\begin{aligned} X &= 2\bar{p}_X \approx A\cos(\theta), \\ Y &= 2\bar{p}_Y \approx A\sin(\theta). \end{aligned} \tag{7}$$

The measurement method proposed in this paper consists of injecting a very low-frequency signal to the stator. An embedded digital LIA measures the current and voltage of this signal. These measurements are used to compute the stator resistance and then to estimate the motor temperature.

Fig. 1 shows an induction motor steady-state equivalent circuit. The proposed method does not use this model to estimate temperature; the equivalent circuit is only used in this section to study the method. The stator is fed by two voltage sources with different frequencies, the power supply (V_P) and the monitoring signal (MS) voltage source (V_M).

In order to make most of the stator current flow through the magnetizing inductance (L_M), the MS frequency must be low enough. Mathematically

$$|j\omega_M L_M| \ll \left|\frac{R_R}{s_M} + j\omega_M L_{LR}\right| \tag{8}$$

where ω_M is the MS frequency, L_M is the magnetizing inductance, R_R is the rotor resistance, L_{LR} is the stator leakage inductance, and s_M is the normalized slip frequency measured with respect to the MS. This relation can be satisfied by selecting a very low ω_M, making its validity independent of the motor parameters.

If this condition is satisfied, the equivalent stator impedance at frequency ω_M, seen at the motor terminals, is as follows:

$$Z_S(\omega_M) \approx R_S + j\omega_M L_S \tag{9}$$

where

$$L_S = L_M + L_{LS}. \tag{10}$$

The adequate ω_M value depends on the machine electrical parameters, and in general, a correct choice is 0.1 Hz or lower. Fig. 2 shows the R_S measurement error using the approximation (9) as a function of the MS frequency (ω_M) and the normalized slip (i.e., different rotor speeds) for a motor whose parameters are shown in the Appendix. For dc injection ($\omega_M = 0$), the error is zero for any slip. For very low frequencies (i.e., $\omega_M < 0.1$ Hz), the error is low enough for temperature monitoring applications (<1%). If the MS frequency is lower, the measurement time is higher and the time response can be too slow to detect fast temperature changes.

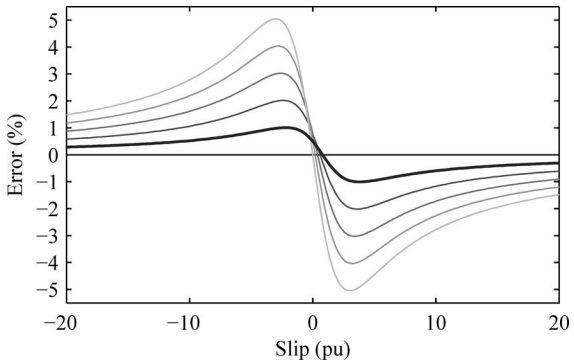

Fig. 2. Expected R_S measurement error as a function of slip (normalized with respect to ω_M, with different MS frequencies (from 0 to 0.5 Hz). Lighter lines indicate higher frequencies. The selected frequency is indicated with a thicker line.

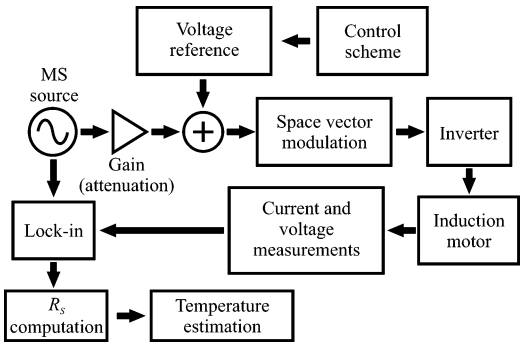

Fig. 3. Proposed temperature monitoring system block diagram.

A block diagram of the proposed scheme is shown in Fig. 3. The lock-in amplification technique is used to measure the voltage and current signals at frequency ω_M. From these values, the stator resistance is computed, and the average stator windings temperature is estimated. The stator resistance is computed as follows:

$$R_S \approx \mathrm{Re}\left\{Z_S\left(\omega_M\right)\right\} = \mathrm{Re}\left\{\frac{V_M}{I_M}\right\} = \frac{V_X I_X + V_Y I_Y}{I_X^2 + I_Y^2} \quad (11)$$

where the subindexes X and Y represent the real and imaginary parts of the signals, V_M and I_M are the MS voltage and current measurements, respectively, obtained by using the lock-in technique.

If the MS frequency is low enough, the imaginary parts can be neglected ($I_Y \ll I_X$) and (11) can be approximated to reduce the computational requirements

$$R_S \approx \frac{V_X}{I_X}. \quad (12)$$

In the prototype presented in Section III, the MS frequency is 0.1 Hz and it was experimentally verified that (12) is valid.

B. Injected Signal Effects

Any injected MS used to monitor the motor temperature has negative incidence in motor operation. The main effects are additional power dissipation in the motor windings, torque ripple and braking torque. Considering the equivalent circuit of Fig. 1, these effects can be predicted.

In Fig. 1, the stator is fed by two voltage sources, the power supply (V_P) and the MS source (V_M). At constant speed, the equivalent circuit is a linear system. Hence, superposition can be applied to analyze individually the power supply and MS currents.

The stator current is given by

$$I_S\left(\omega\right) = \frac{V_S\left(\omega\right)}{Z_S\left(\omega\right)} \quad (13)$$

where I_S and V_S are the stator current and voltage, respectively, and Z_S is the equivalent stator impedance, which is given by

$$Z_S(\omega) = R_S + j\omega L_{LS} + \frac{1}{(1/j\omega L_M) + (1/(R_R/s_\omega + j\omega L_{LR})}. \quad (14)$$

From the stator current, the rotor current can be computed as follows:

$$I_R\left(\omega\right) = I_S\left(\omega\right)\frac{jL_M}{R_R/(\omega - \omega_R) + jL_R} \quad (15)$$

where ω_R is the rotor electrical speed. From both currents, the electromagnetic torque, as a function of time, is given by [2]

$$T_e(t) = \frac{3}{2}\frac{np}{2}L_M\left(i_{qs}(t)i_{dr}(t) - i_{ds}(t)i_{qr}(t)\right) \quad (16)$$

where *np* is the pole number. The motor currents are denoted by $i(t)$. Subindexes s and r indicate stator and rotor, d and q indicate the quadrature axes in the stationary reference frame. Each current is composed by the sum of the power supply current and the MS current

$$\begin{aligned} i_{ds}(t) &= A_{Ps}\sin(\omega_P t + \theta_{Ps}) + A_{Ms}\sin(\omega_M t + \theta_{Ms}),\\ i_{qs}(t) &= A_{Ps}\cos(\omega_P t + \theta_{Ps}) + A_{Ms}\cos(\omega_M t + \theta_{Ms}),\\ i_{dr}(t) &= A_{Pr}\sin(\omega_P t + \theta_{Pr}) + A_{Mr}\sin(\omega_M t + \theta_{Mr}),\\ i_{qr}(t) &= A_{Pr}\cos(\omega_P t + \theta_{Pr}) + A_{Mr}\cos(\omega_M t + \theta_{Mr}) \end{aligned} \quad (17)$$

where the amplitudes and phases are defined by

$$\begin{aligned} A_{yx} &= |I_y(\omega_x)|,\\ \theta_{yx} &= \arg[I_y(\omega_x)] \end{aligned} \quad (18)$$

the subindexes P and M indicate power and monitoring currents, respectively.

As a result of the different frequency components, the electromagnetic torque (16) has a dc component, and an ac component with a frequency equal to the difference between the two current frequencies. Hence, the torque can be expressed as follows:

$$T_e(t) = \frac{3}{2}\frac{np}{2}L_M\left(T_{\mathrm{dc}} + T_{\mathrm{ac}}(t)\right). \quad (19)$$

The ac component produces torque ripple. This ripple can produce a significant speed ripple if the load inertia or the ripple frequency are not high enough.

The dc component is composed by the sum of the torques produced by both frequencies. If the machine is working as a motor, the low-frequency current has a negative slip. Hence,

TABLE I
INFLUENCE OF THE MS AMPLITUDE

MS voltage	Braking torque	Torque ripple	Power losses
0.05 pu	5.62E-3 pu	0.2 pu	5.22E-2 pu
0.005 pu	5.62E-5 pu	0.02 pu	5.22E-4 pu

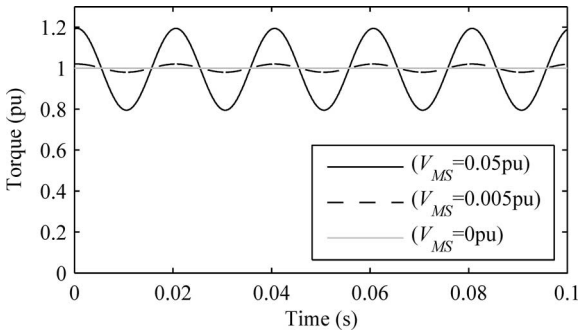

Fig. 4. Simulation of the electromagnetic torque with different MS amplitudes.

the torque produced by the MS is negative and it counteracts the positive torque produced by the power supply current. This property is used as braking technique in many applications.

The additional power dissipation generated by the MS is another negative effect of signal injection methods. The MS stator current increases the stator winding losses. Furthermore, the negative torque component produces a mechanic power dissipated in the rotor resistance. Considering that the MS frequency is very low, the additional power dissipated by the MS in the stator and rotor resistances is as follows:

$$\Delta P = I_{SM}^2 R_S + I_{RM}^2 R_R \tag{20}$$

where I_S and I_R are given by (13)–(15), and the M subindex indicates the MS components of both currents.

In Table I and Fig. 4, the effects for different MS amplitudes are compared. The MS voltage used in the implementation presented in this paper is 0.005 pu, the value used in implementations that use dc injection is generally higher than 0.05 pu (e.g., [12]–[14]).

Fig. 4 shows a simulation of the electromagnetic torque in steady state using a model of the machine described in the Appendix. If the MS amplitude is not low enough, the torque ripple can be significant (0.2 pu peak). In Table I, the braking torque, torque ripple, and additional power losses are compared. Power losses are normalized with respect to the total resistive power losses without signal injection.

Another secondary effect produced by the injected signal is an eventual increment in the magnetic saturation of the machine. This saturation cannot be predicted using the linear induction motor model. However, if the MS level is low enough (i.e., its current is much lower than the nominal current), its effects on machine saturation are negligible.

The arguments presented in this section show the necessity of reducing the MS amplitude in order to minimize its negative effects.

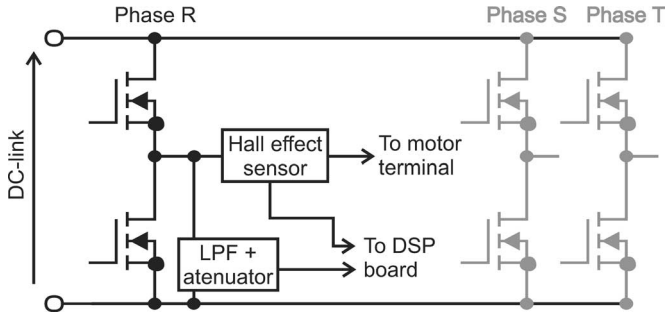

Fig. 5. Schematic diagram of the electric variables measurement for one of the three inverter phases.

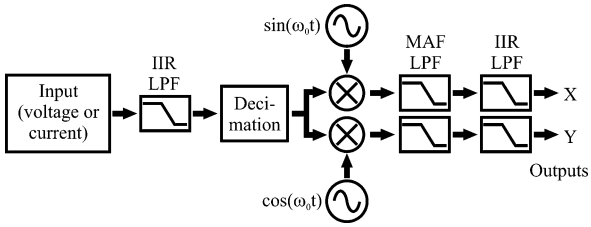

Fig. 6. Embedded LIA simplified block diagram.

IV. PROTOTYPE DESCRIPTION

The proposed temperature monitoring method was validated in a DSP-based motor drive. The processing unit is a TMS320F2812 DSP. The power stage is composed of a MOSFET inverter operating with a dc-link voltage of 42 V. The experimental results are taken in a 1.25 kW, low-voltage induction machine, whose parameters are given in the Appendix. Fig. 3 shows a simplified block diagram of the complete system.

The phase currents are measured using Hall effect sensors. The three phase voltages are individually measured with respect to inverter ground. Low-pass filters (LPF) are used to filter-out the switching harmonics. Fig. 5 shows a schematic diagram of the electric variables measurement. The phase-to-phase voltages are computed by the DSP software. The temperature monitoring accuracy depends on the voltage and current measurements. Phase voltage or current reconstruction from the inverter states and dc-link measurements [16] may not be accurate enough because inverter nonlinearities (e.g., commutation times and dead-times) significantly distort low-voltage signals [17].

The MS can be injected to the motor as stator current injection or stator voltage injection, because the proposed method measures both variables. The implemented prototype uses a scalar V/f controller [2]. A low-amplitude (0.005 pu) and low-frequency (0.1 Hz) MS is added to the controller reference voltage (voltage injection). In case of field-oriented controlled drives, the MS should be added to the stator current reference in the stationary reference frame [2] (current injection).

From the phase current and voltage measurements, the real and imaginary components of the motor impedance at the MS frequency are computed using the lock-in technique. Fig. 6 shows a block diagram of the measurement stage using this method.

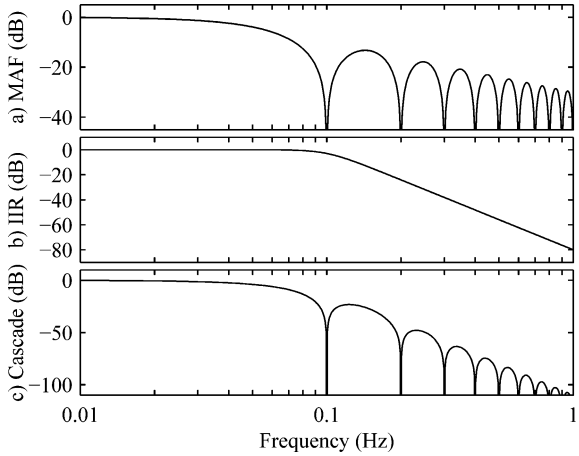

Fig. 7. Ideal frequency response magnitudes of the filters used in the digital signal processing stage.

The input signals sampling is synchronized with the pulsewidth modulation commutations (at 20 kHz in this implementation) to reduce the switching noise. An excessively high sampling frequency, compared with the filters' cutoff frequency, increases the implementation complexity of digital filters due to truncation errors [18]. In the implemented drive, the sampling frequency of the embedded LIA is divided by an integer factor (decimation) in order to simplify the implementation of filters with very low cutoff frequency using 32-bit fixed-point arithmetic. An infinite impulse response (IIR) LPF is used, previous to decimation, to avoid aliasing with high-frequency signals (e.g., power supply current).

The LPF stage of Fig. 6 is composed of two types of cascaded filters. A moving average filter (MAF) is used to eliminate the fundamental ac frequency and its harmonics. The MAF duration is made equal to the MS period, thus the filter frequency response has "zeros" at the MS frequency and its harmonics [18]. The IIR filter has a frequency response more suitable to attenuate the rest of the spectrum, specially the power supply current and switching ripple. Fig. 7 shows the ideal MAF, IIR, and cascaded filters frequency responses.

Multiplications (5) and (6) performed by the lock-in generates the following four frequency components.

1) DC component, whose value must be measured in (7).
2) A component with $2\omega_M$ frequency, which must be filtered-out (mainly by the MAF filter).
3) A component with ω_M, coming from the current and voltage measurements offset, which must also be filtered-out (mainly by the MAF filter).
4) Components of frequencies $\omega_P \pm \omega_M$, produced by intermodulation with the power supply waveform. If $\omega_P > \omega_M$, these components will be filtered-out (mainly by the IIR filter). When ω_P is very low (i.e., $\omega_P \approx \omega_M$), the power signals (voltages and currents) will not be completely filtered out. In this case, the power signals contribute to the R_S measurement in the same way as the MS, because they have very low frequency and (8) is valid. The first experimental test (see Section V) shows the correct operation in this regime. Temperature estimations have lower fluctuations than the other tests because measurements are based on a much greater signal (the power supply current).

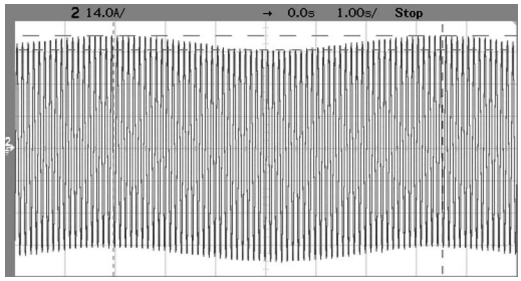

Fig. 8. Oscilloscope capture of a phase current. The low-amplitude MS is added to the fundamental power supply current.

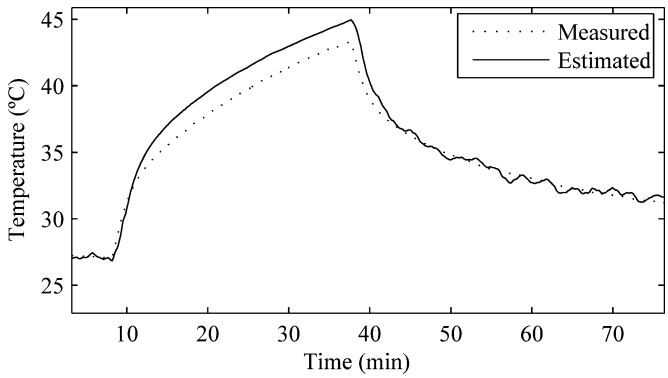

Fig. 9. Stator temperature temporal evolution. An 80-mHz speed step is applied at $t = 9$ min. At $t = 38$ min, the power supply current is turned off.

After the ac components are filtered out, four dc values that represent the real and imaginary components of the MS current and voltage are obtained. From these measurements, the R_S value is computed using (11) [or its approximation, (12)] and the temperature is estimated using (1).

V. Experimental Results

The experimental tests performed with the prototype consist of running the motor under different operating conditions. The temperature estimated using the proposed method is compared with a sensor measurement. The temperature sensor is an integrated circuit (LM35) placed inside one of the stator windings. Fig. 8 shows an oscilloscope capture of one phase current, composed by the fundamental power supply current added to the low-level and low-frequency MS signal.

In Figs. 9–11, the results obtained for different rotor speeds are shown. At the beginning, the motor is at room temperature in steady state. In Fig. 9, an 80 mHz speed reference is applied at $t = 9$ min. A significant temperature rise is produced because the cooling system does not operate correctly at very low rotor speeds (the fan is coupled to the rotor). The power supply current is turned off at $t = 38$ min, initiating an exponential temperature decrement down to room temperature. The plot shows that the temperature estimation follows

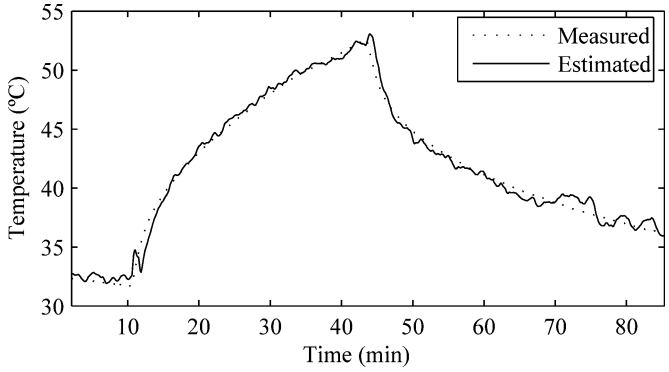

Fig. 10. Stator temperature temporal evolution. A 125 Hz speed step is applied at $t = 10$ min. At $t = 44$ min the power supply current is turned-off.

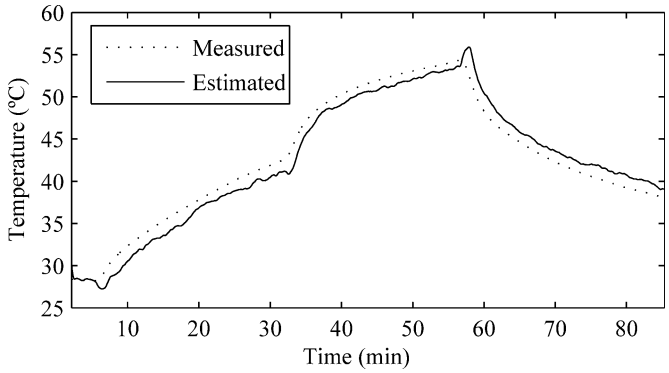

Fig. 11. Stator temperature temporal evolution. A 40-Hz speed step is applied at $t = 6$ min, and at $t = 33$ min the speed is reduced to 4 Hz. At $t = 57$ min, the power supply current is turned off.

correctly the actual temperature. It must be taken into account that the estimated temperature is the stator windings average temperature, and the measured temperature is obtained using a sensor placed inside one of the stator windings. Comparisons between stator resistance-based estimations and temperature measured in different locations of stator windings can be found in the literature [5], [15].

The sequence for Fig. 10 is similar to Fig. 9, but with a 125 Hz speed reference (near 1.5 times nominal speed). In Fig. 11, a 40 Hz speed reference step is applied at $t = 6$ min, then the speed is reduced to 4 Hz at $t = 33$ min. This rotor speed reduction also reduces the motor ventilation, thus incrementing the motor temperature, as shown in the plot. The power supply current is turned off at $t = 57$ min.

In the presented results, the maximum estimation error is near 2.5 °C (less than 1% error in the R_S measurement), which satisfies the monitoring requirements stated at the beginning of this paper. Furthermore, temperature estimations can be used to compensate the model parameters used in high-performance controllers. It is worth noticing that the experimental tests include speed and current transients. This shows that the proposed method is valid for any operating condition.

VI. Conclusion

A method that estimates the internal temperature of induction motors, without using additional sensors, was proposed in this paper.

The method injects a low-level signal to the stator windings in order to measure their electric resistance. The proposed method has advantages with respect to the other methods found in literature. The measurement technique, which uses ac signals instead of dc signals, allows a significant reduction of the MS amplitude without affecting its accuracy, even in presence of high offset, drift, or noise in the analog circuits. Hence, the proposed measurement technique solves the main problem found in previous publications related to dc signal injection.

It is mathematically demonstrated that the MS level reduction allows a significant decrement in torque distortion and additional power losses.

The experimental results show that the proposed method is able to accurately estimate the stator temperature in the whole motor speed range, even in current and speed transients, and in field weakening region (very high speed). The reported maximum estimation error is 2.5 °C.

The mathematical analysis and the experimental prototype presented in this paper are applied to induction machines. However, the proposed technique is applicable to other types of ac machines, such as synchronous or brushless machines.

It is worth noticing that although in this paper the signal injection method is implemented using the motor drive inverter, the same technique can be applied to line-connected motors by using external devices. The only modification to the external device proposed in [5] and [10] can be implemented by software. Instead of injecting a dc offset in one motor phase, the injected component must be a low-frequency ac. The digital signal processing complexity required for the technique implementation is low, and it does not need high-speed microprocessors.

Appendix

TABLE II
Induction Motor Electric Parameters Used for the Experimental Tests and the Simulations

Parameter	Value
Nominal power	1.25 kW
Nominal voltage	25.4 V_{RMS}
Nominal frequency	83,3 Hz
R_S	56 mΩ
R_R'	15,7 mΩ
L_M	1,65 mH
$L_{LR'}$=L_{LS}	95 μH

References

[1] A. H. Bonnett and G. C. Soukup, "Cause and analysis of stator and rotor failures in three-phase squirrel-cage induction motors," *IEEE Trans. Ind. Appl.*, vol. 28, no. 4, pp. 921–937, Jul. 1992.

[2] R. Krishnan, *Electric Motor Drives: Modeling, Analysis and Control*. Englewood Cliffs, NJ: Prentice-Hall, 2001.

[3] J. T. Boys and M. J. Miles, "Empirical thermal model for inverter-driven cage induction machines," *Inst. Electr. Eng. Proc. Electr. Power Appl.*, vol. 141, no. 6, pp. 360–372, 1994.
[4] Z. Lazarevic, R. Radosavljevic, and P. Osmokrovic, "A novel approach for temperature estimation in squirrel-cage induction motor without sensors," *IEEE Trans. Instrum. Meas.*, vol. 48, no. 3, pp. 753–757, Jun. 1999.
[5] S. B. Lee and T. G. Habetler, "A remote and sensorless thermal protection scheme for small line-connected AC machines," *IEEE Trans. Ind. Appl.*, vol. 39, no. 5, pp. 1323–1332, Sep./Oct. 2003.
[6] P. Milanfar and F. H. Lang, "Monitoring the thermal condition of permanent-magnet synchronous motors," *IEEE Trans. Aerosp. Electron. Syst.*, vol. 32, no. 4, pp. 1421–1429, Oct. 1996.
[7] Ch. Kwon and S. D. Sudhoff, "An on-line rotor resistance estimator for induction machine drives," in *Proc. IEEE Int. Conf. Electr. Mach. Drives*, 2005, pp. 392–397.
[8] M. O. Sonnaillon and F. J Bonetto, "A low cost, high performance, DSP-based Lock-In amplifier capable of measuring multiple frequency sweeps simultaneously," *Rev. Sci. Instrum.*, vol. 76, pp. 024703-1–024703-7, 2005.
[9] H. Kubota, K. Matsuse, and T. Nakano, "DSP-based speed adaptive flux observer of induction motor," *IEEE Trans. Ind. Appl.*, vol. 29, no. 2, pp. 344–348, Mar. 1993.
[10] S. B. Lee, T. G. Habetler, R. G. Harley, and D. J. Gritter, "An evaluation of model-based stator resistance estimation for induction motor stator winding temperature monitoring," *IEEE Trans. Energy Convers.*, vol. 17, no. 1, pp. 7–15, Mar. 2002.
[11] Y. Wu and H. Gao, "Induction-motor stator and rotor winding temperature estimation using signal injection method," *IEEE Trans. Ind. Appl.*, vol. 42, no. 4, pp. 1038–1044, Jul./Aug. 2006.
[12] D. Holliday, T. C. Green, and B. W. Williams, "On-line measurement of induction machine stator and rotor winding parameters," in *Proc. Inst. Electr. Eng. Power Electron. Variable Speed Drives*, 1994, pp. 465–469.
[13] L. A. De Souza Ribeiro, C. B. Jacobina, and A. M. Nogueira Lima, "Linear parameter estimation for induction machines considering the operating conditions," *IEEE Trans. Power Electron.*, vol. 14, no. 1, pp. 62–73, Jan. 1999.
[14] M. Stiebler and Y. Plotkin, "Online winding temperature monitoring of PWM inverter-fed induction machines," in *Proc. Eur. Conf. Power Electron. Appl.*, 2005, pp. 1–5.
[15] S. B. Lee and T. G. Habetler, "An online stator winding resistance estimation technique for temperature monitoring of line-connected induction machines," *IEEE Trans. Ind. Appl.*, vol. 39, no. 3, pp. 685–694, May/Jun. 2003.
[16] M. O. Sonnaillon, G. Bisheimer, C. De Angelo, J. Solsona, and G. O. García, "Mechanical-sensorless induction motor drive based only on DC-link measurements," *Inst. Electr. Eng. Electr. Power Appl.*, vol. 153, no. 6, pp. 815–822, 2006.
[17] J. Holtz and J. Quan, "Sensorless vector control of induction motors at very low speed using a nonlinear inverter model and parameter identification," *IEEE Trans. Ind. Appl.*, vol. 38, no. 4, pp. 1087–1095, Jul./Aug. 2002.
[18] S. W. Smith. (1999). *The Scientist and Engineer's Guide to Digital Signal Processing* (*2nd ed.*) [Online]. Available: http://www.dspguide.com

Maximiliano O. Sonnaillon (M'07) was born in Paraná, Argentina, in 1979. He received the degree (*cum laude*) in electronics engineering from the National Technological University, Argentina, in 2002, the M.Sc. degree in electrical engineering from the National University of Rio Cuarto, Rio Cuarto, Argentina, in 2005, and the Ph.D. degree in engineering from Balseiro Institute, Bariloche, Argentina, in 2007.

He is currently a Senior Research and Development Engineer for Elgar Electronics, San Diego, CA, where he develops advanced programmable power supplies based on digital control and state-of-the-art power electronics. His research interests include digital signal processing, control systems, electric machines, and power electronics.

Dr. Sonnaillon received the National Award "Prize to the Best Graduates in Engineering at Argentine Universities", from the National Academy of Engineering, Argentina, in 2003.

Guillermo Bisheimer was born in Paraná, Argentina, on June 14, 1979. He received the degree in electronics engineering from the National Technological University, Argentina, in 2002, and the M.Sc. degree in electrical engineering from the National University of Rio Cuarto, Rio Cuarto, Argentina, in 2006. He is currently working toward the Ph.D. degree in the Department of Electrical and Computer Engineering, University of the South, Bahia Blanca, Argentina.

His current research interests include high-performance motor drive systems, power electronics, digital electronics, and digital signal processing applications to electrical machines characterization and fault diagnosis.

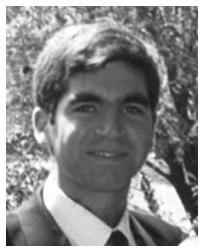

Cristian De Angelo (S'96–M'05) received the degree in electrical engineering from the National University of Rio Cuarto, Rio Cuarto, Argentina, in 1999, and the Dr. of Engineering degree from the Universidad Nacional de La Plata, La Plata, Argentina, in 2004.

In 1994, he joined the Applied Electronics Group, National University of Rio Cuarto. He is also currently with the Consejo Nacional de Investigaciones Científicas y Técnicas. His research interests include sensorless motor control, fault diagnosis in electric drives, power electronics, electric vehicles, and renewable energy generation.

Dr. De Angelo is a member of the Automatic Control Association of Argentina.

Guillermo O. García (M'86–S'90–SM'01) received the degree in electrical and electronics engineering from the National University of Cordoba, Cordoba, Argentina, in 1981, the M.Sc. and Ph.D. degrees in electrical engineering from COPPE, Federal University of Rio de Janeiro, Rio de Janeiro, Brazil, in 1990 and 1994, respectively.

In 1994, he joined the National University of Rio Cuarto, Rio Cuarto, Argentina, where he is the Director of the Applied Electronics Group, a Coordinator of a Graduate Program in Electrical Engineering, and a Professor in the Electrical and Electronics Department. He was engaged in several R&D projects, at universities and industries. He is also member of the National Research Council (Consejo Nacional de Investigaciones Científicas y Técnicas). His current research interests include power electronics, motion control, electric vehicles renewable energy conversion, and industrial automation and control.

Dr. García is also engaged to the the professional societies: the IEEE Industry Applications, Industrial Electronics, Power Electronics, Control Systems, Power Engineering and Education, and the Argentina Automatic Control Association.